PERMEABILITY OF MEMBRANE JUNCTIONS*

Werner R. Loewenstein
Cell Physics Laboratory, Department of Physiology, Columbia University, College of Physicians and Surgeons, New York, N. Y.

Introduction

The general and familiar idea of the cell membrane is that of a barrier to diffusion encompassing the entire cell surface. This idea derives largely from work with a few cell types: nerve, striated muscle, blood, and gamete cells. These are, however, rather peculiar cells. They are generally not in direct contact with each other but are separated by wide fluid-filled spaces. I shall deal here with the question of what happens to the diffusion barrier when two cell membranes are brought close together. This states the question for the general case of cell association; most tissues, by far, are built of cells in close surface contact.

I chose epithelial cells for a study of this question. These cells have several advantages. Their areas of membrane contact are large, and their size permits direct conductance measurements. The giant salivary gland cells of *Drosophila* and *Chironomus* were particularly suitable in this respect (FIGURE 1).

Intercellular Ion Continuity

FIGURE 2 illustrates the experiment that was the starting point. Three microelectrodes are inserted into two adjacent cells of a *Drosophila* gland. One serves to pass current between the cell interior and the exterior, and the other two to record the resulting voltage drops across the cell membranes. The cell membranes in these cells behave like fairly good ohmic resistors; they show little or no rectification and no signs of electrical activity over a wide range of current. The striking result is that the resistive membrane voltages for any given current are nearly the same in the two cells.

Three things are immediately clear from the result of this simple experiment: (1) The electrical resistance of the surface membrane (r_o, FIGURE 3) bordering the exterior is high. This obviously is the membrane that must sustain the high voltage; the slope of the current-voltage curve is of the order of 10^5 Ω. (2) The resistance across the junctional membranes, r_c, is much lower than that of the surface resistance, r_o. Clearly, a large fraction of the current must have flowed through the junctional membranes to give so small an attenuation of voltage. (3) The resistance r_s, from a cell interior to the exterior via the junctional surfaces (referred to hereafter as *intercellular space resistance*), is relatively high. This, too, follows from the low attenuation of voltage.

These points are further illustrated by the experiment described in FIGURE 4. Current is passed from an electrode fixed in one cell, and the resulting membrane voltages are recorded with a roving electrode from inside cells located at varying distances from the current source. Membrane voltage decreases with distance, but the decrement is only of an order one would expect if the gland, with its 200 cells, were to behave like a cable conductor with a continuous cytoplasmic core bounded solely by an external insulating membrane. In fact, in those cases in which the gland diameter was small in relation to the space constant of voltage

* Part of the work reported in this paper was supported by research grants of the National Science Foundation and the National Institutes of Health.

decrement, and in which there were no appreciable voltage drops in the radial dimension of the gland, agreement with cable theory was fairly good (Loewenstein & Kanno, 1964). For example, in a representative case of a gland of 200 μ diameter, the space constant was 1.2 mm., which happens to be practically the same as in squid giant axon, in which there are clearly no partitions in the cytoplasmic core equivalent to junctional membranes, nor leakage paths equivalent

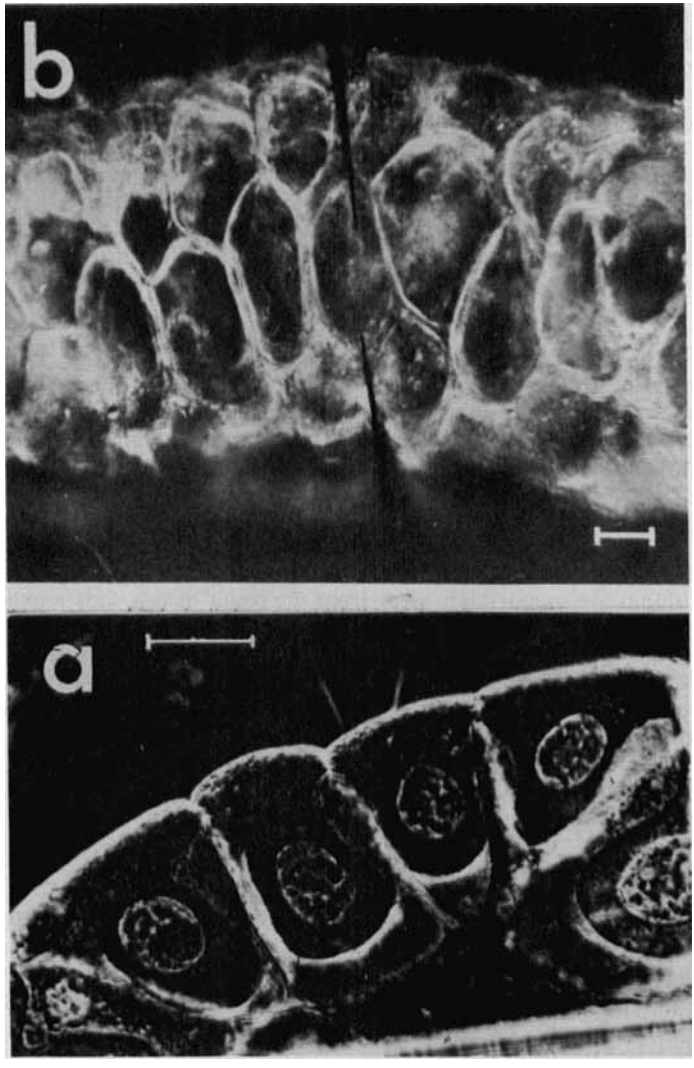

FIGURE 1. Darkfield views of a *Drosophila* (*b*) and a *Chironomus* (*a*) salivary gland. The tips of two microeletrodes (retouched in *b*) are seen in one cell. Calibration, 50 μ. (From Loewenstein & Kanno, 1964.)

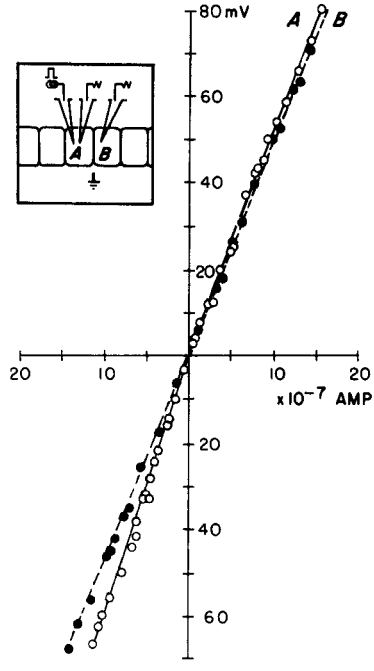

FIGURE 2. Junctional communication (*Drosophila* salivary gland). Current (*abscissae*) is passed between a microelectrode inside cell *A* and the extracellular fluid (grounded) and the resulting drops in resistive membrane voltage (*ordinates*) are recorded inside cells *A* and *B*. Outward current, *right*; depolarization, *upwards*. (From Loewenstein & Kanno, 1964.)

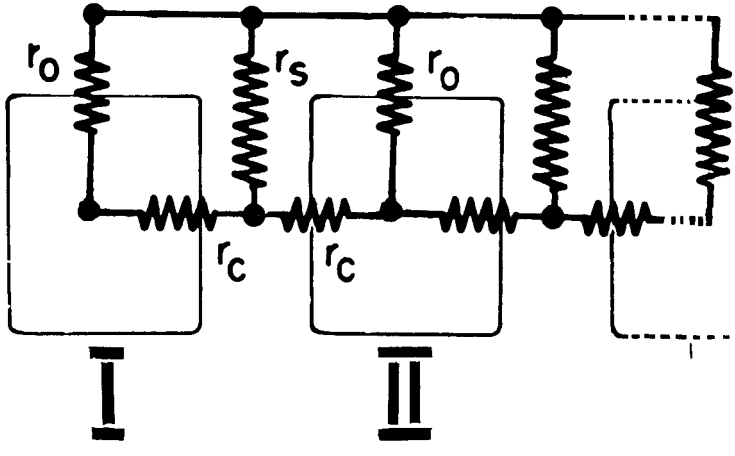

FIGURE 3. Equivalent circuit of a cell chain. r_o, resistance across the cell surface membrane; r_c, across the junctional membrane; r_s, along the intercellular space to the exterior, that is, between a central point of the interconnection and the exterior.

to intercellular spaces. This shows again that the junctional membranes offer low resistance to ion flow and that the intercellular space resistance is high.

Junctional Membrane Conductance

Linear transmission line analysis of experiments of voltage attenuation, such as those in FIGURE 4, allows one to obtain values of surface resistance (r_m) and core resistance (r_i). We are dealing here with a somewhat unusual transmission line. Its length is only slightly greater than its space constant. Thus the (single) exponential expression for spatial distribution of potential, which has been so frequently useful in dealing with nerve and muscle fibers (Hodgkin & Rushton, 1946), is not sufficient here. If the current source is at the midpoint or at one end of the core conductor, an expression that satisfies the differential equation and the boundary conditions is:

$$V = V_o \frac{\cosh\frac{L - x}{\lambda}}{\cosh\frac{L}{\lambda}} \tag{1}$$

where V, the resistive voltage across the gland surface, is proportional to a hyperbolic cosine function of x, the distance along the gland axis from the current source. V_o is V at $x = 0$; L, the gland length; and λ, the space constant. The resistance of unit surface, R_m, is then:

$$R_m = \left(\frac{\lambda V_o}{I_o} \tanh\frac{L}{\lambda}\right) \cdot p \tag{2}$$

and the core resistance, R_i:

$$R_i = \left(\frac{V_o}{\lambda I_o} \tanh\frac{L}{\lambda}\right) \cdot a \tag{3}$$

where I_o is the total input current, p the gland circumference, and a the cross-sectional area (Loewenstein & Kanno, 1964).

Analysis of data of resistive voltage attenuation leads thus to values of the order of 10^4 Ω cm.^{2} for surface resistance, R_m (corrected for surface infoldings as seen in electron micrographs); and of 110–190 Ω cm. for the core resistance, R_i, that is, the resistance of the cytoplasm-junctional membrane complex in the axial direction of the system. The value of surface resistance is of the same order as that of a wide variety of cell membranes. The novel result is the low resistance of the cytoplasm-junctional membrane complex which does not amount to much more than that of cytoplasm alone.

The resistance of the cytoplasm-junctional membrane complex may be determined also by direct measurement (FIGURE 5). In these measurements, the cell exterior is bypassed effectively by bathing the cell system in a medium of high resistivity (sucrose, oil), and current flows from cytoplasm to cytoplasm across a series of membrane junctions. The measured resistance increases roughly linearly with the length of the cell chain through which the current is flowing; the slope of the curve corresponds to a resistance of 160 Ω cm. This value fits well with that obtained above by transmission line analysis. Since extruded gland cytoplasm has a resistivity of 100 Ω cm. alone, it is clear that the junctional membranes do not present substantial barriers to ion flow.

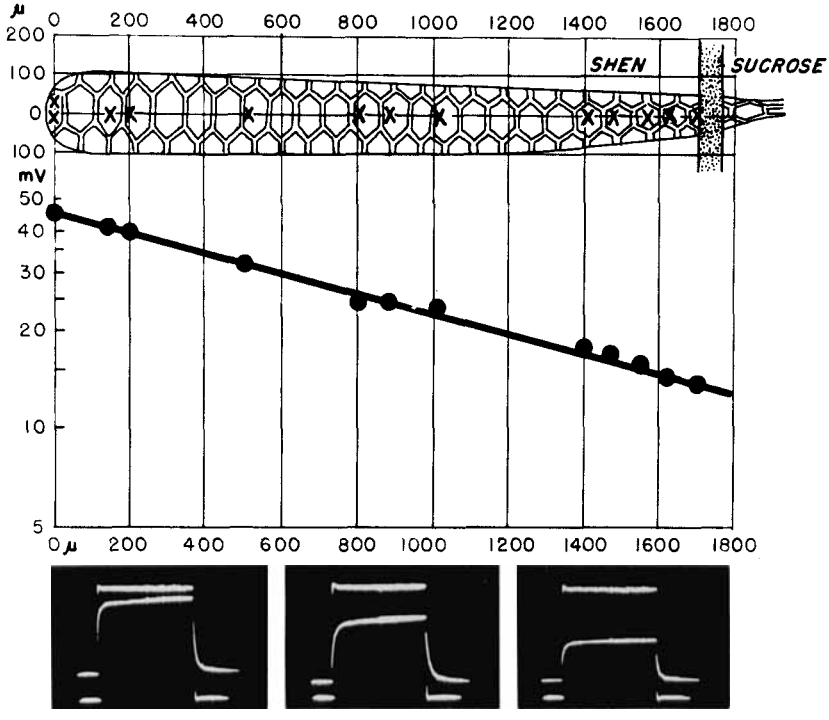

FIGURE 4. Cell communication throughout a gland epithelium (*Drosophila*). Current is passed between a microelectrode in one cell (length 0 on *abscissae*) and the exterior, and the resulting resistive membrane voltages (*ordinates*) are recorded across the membranes of cells located at varying distances (*abscissae*) from the current-passing microelectrode. Gland duct filled with sucrose to avoid current leakage through the luminal cell surface. *Upper inset*, camera lucida drawing of the gland epithelium; the crosses denote points of electrode insertion. *Lower inset*, samples of records of membrane current (upper beam) and membrane voltage (lower beam) at 0, 200, and 800 μ. Current pulse duration, 60 msec. (From Loewenstein & Kanno, 1964.)

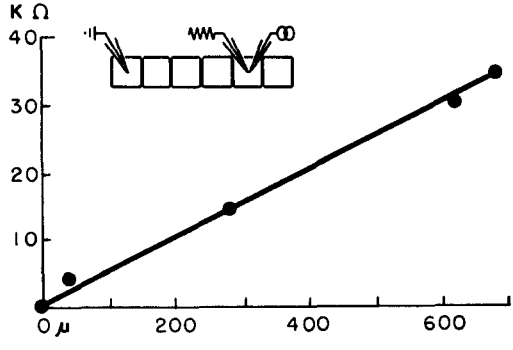

FIGURE 5. Resistance of the junctional membrane-cytoplasm complex. Resistance (*ordinates*) measured along the interior of a cell chain between an electrode (⊥) inside a cell and a roving electrode inserted into cells at varying distances (*abscissae*) along the chain. Ordinates give the resistance after subtraction of the resistance of the measuring electrode (⊥), constant within 2 K Ω. (From Loewenstein & Kanno, 1964.)

Junctional Membrane Permeability

The core resistance of the system, 150 Ω cm., is so low that, even a priori, there are no serious doubts that the specific membrane resistance, that is, the membrane permeability at the junctional surfaces is very different from that of the rest of the cell surfaces. There is simply no room at the junction to account for so low a core resistance on the basis of a large junctional surface alone with permeability characteristics of the surface membrane. Consider, for instance, a hypothetical junctional membrane packing in which there is a membrane every 100 Å, a packing so efficient that there is virtually neither cytoplasm nor gap between membrane folds. Even in such an absurdly dense packing, and allowing for maximal junctional space and depth of infolding, the surface area falls short by two orders of magnitude from that required to give the measured core resistance (Loewenstein & Kanno, 1964).

The question may be examined more rigorously with the aid of electron micrographs from which an upper limit of the total junctional membrane surface is obtained. This limit lies between 10^{-4} and 10^{-3} cm.^{2} (Wiener *et al.*, 1964) and gives an upper limit of 10 Ω cm.^{2} for the junctional membrane resistivity. The actual value is likely to be even lower (0.1 to 1 Ω cm.^{2}), since for the estimate of the upper limit the total cell contact area was used, which includes both the convoluted and septate regions of the junction (see below).

In conclusion, the membranes that function as junctional elements between cells have ion permeabilities at least four orders of magnitude greater than those of the non-junctional surface membranes.

Surface Membrane Permeability

The surface resistance of the system, 10^4 Ω cm.^{2}, is the parallel combination of the resistance of the cell surface membrane (r_o, FIGURE 3) and the resistance (r_s) from cell interior to exterior through the junctional surface. Both are clearly of a high order of magnitude; the lower limit for both is 10^4 Ω cm.^{2} In the experiment illustrated in FIGURE 6, an attempt is made to resolve further between the two by a method of high space resolving power and one that does not rely on cable conductor properties of the cell system alone. The large *Drosophila* gland cells offer the unusual opportunity to record membrane voltage from several spots of a given cell surface. The potential field around a point source of current is probed here at various points along the inside of the surface membranes of adjacent cells; pairs of successive points occur both on a single cell and straddling a cell junction. The object was to see whether there is a greater current leak at the level of the junction than at the surface membrane. The answer was clearly, no. All voltage points fall sensibly along a simple smooth curve, regardless of whether they are recorded on the edge of a junction or at a central spot of the cell surface.

Scheme of a Communicating Cell System

FIGURE 7 gives a schematic picture of cell communication as it emerges from the preceding results: *a cell system with a fairly continuous interior, as far as some of its ion content is concerned, bounded by a diffusion barrier continuous along the entire external surface of the system, including the junctions.* The scheme is, of course, purely functional. The openings in the junctional membranes represent high ion permeability, not coarse interruptions of continuity in membrane structure (see below).

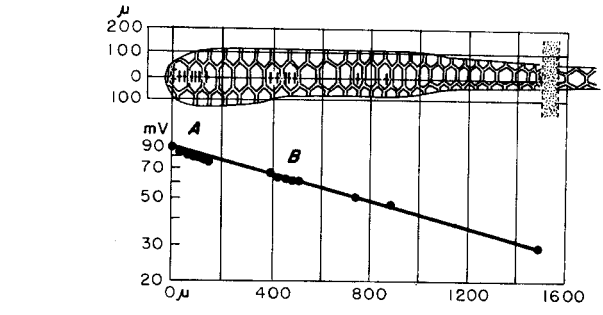

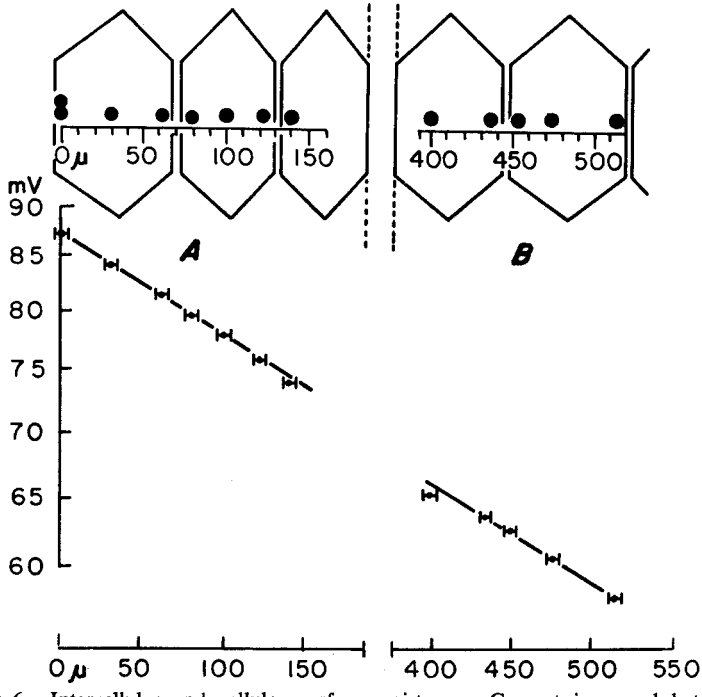

FIGURE 6. Intercellular and cellular surface resistances. Current is passed between an intracellular point (distance 0) and the exterior, and the resulting resistive membrane voltage is recorded intracellularly at a depth of up to 1 μ from the surface membrane at points located near the cell surface centers and at the edges of the cell junctions. *Ordinates,* mean membrane voltage of various successive measurements; standard error less than 0.3 per cent. *Abscissae,* distance; bars subtend standard error. (From Loewenstein & Kanno, 1964.)

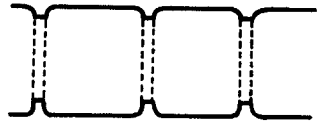

FIGURE 7. Scheme of a connected cell system.

Intercellular Continuity to Larger Particles

The electrical measurements showed that the membranes in the system are so constituted that intracellular ions, at least the small ones, move rather freely from one cell to another, but not to the exterior. Do also larger particles diffuse through the junctional membranes? Information on this point is as yet scant. We have tried a number of molecules and ions as tracers for intercellular diffusion, guiding our choice by size, mobility, and ease of detection of the particles; but only few of them gave reliable results. The difficulty here is to find substances that can be traced in concentrations safe for the cells.

An excellent tracer is fluorescein. Fluorescein has a molecular weight of 332, diffuses readily through cytoplasm, and can be traced by its fluorescence in ultraviolet in concentrations as low as 10^{-8} M. We injected 10^{-9} cc. of a 10-mM. solution of fluorescein-Na with a micropipette into a cell of the *Drosophila* salivary gland. The volume injected amounts to about 1 per cent of the (single) cell volume and must have caused an initial change in cell osmolarity of less than 1 per cent. Such injections had no noticeable damaging effects; the cell transparency, the cell volume, the cell membrane potential and resistance, all remained unaltered.

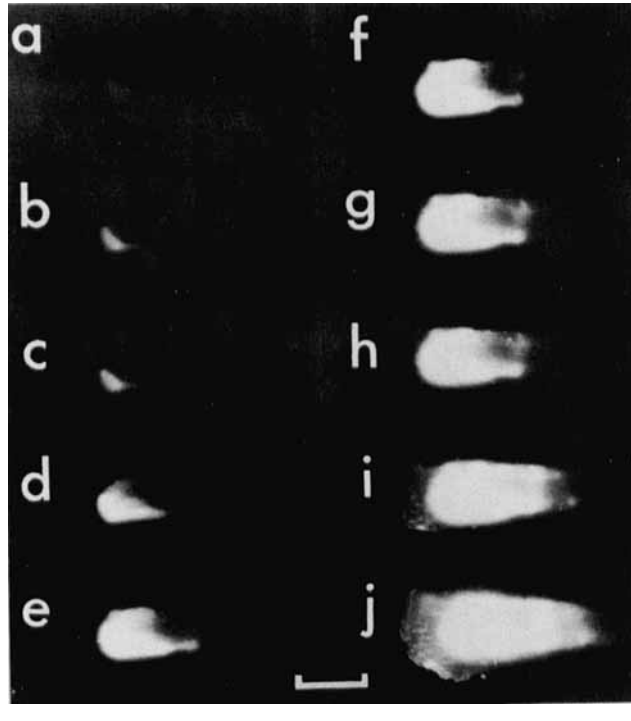

FIGURE 8. Cell-to-cell diffusion. 10^{-9} cc. of fluoroescein-Na are injected into a cell (*Drosophila* salivary gland). Ultraviolet rays are projected obliquely onto the gland, and the scattered fluorescence is photographed at equal exposure time. *a*, at the moment of injection, and *b* to *j*, every 2 minutes after injection. (The differences in intensity of fluorescence are due to fluorescence quenching.) Calibration, 300 μ.

FIGURE 8 illustrates an experiment with fluorescein. Following its injection into the cell, the tracer is seen in the cytoplasm as a fluorescent bleb a few micra in diameter; it spreads progressively through the interiors of this cell and the adjacent ones. Within 5-20 min., depending on the size of the gland, and with constants entirely within the expectations of free diffusion, all cells of the gland, except a few at the duct, become fluorescent.

We tested junctional membrane permeability with a number of other tracer particles, colorant or fluorescent (TABLE 1). They cover a wide span of molecular sizes. The general procedure was to inject 10^{-8}–10^{-9} cc of the tracer solution into a cell and to film its diffusion through the cell system. All tracers summarized in TABLE 1 moved from one cell interior to another with velocities depending on their molecular weight and within expectations of free diffusion; moreover, there were no differences noticeable between their velocities in cytoplasm and at the intercellular boundaries. By contrast, these tracers remained within the boundaries of the injected cells, when the cells were functionally uncoupled by the procedures described below (Kanno & Loewenstein, 1966).

TABLE 1

TRACER MOLECULES DIFFUSING THROUGH MEMBRANE JUNCTIONS

	Molecular Weight	Solution Injected mM
*Azur B (52010)	305	10
†Fluorescein	332	10
*Orange G (16230)	452	22
*Solantine Turquoise (74180)	700	7
*Trypan Blue (477)	960	10
‡Serum albumin	69,000	0.1

* Colorant molecule; Colorant Index No. in parenthesis.

† Fluorescent anion, in solution of its Na-salt.

‡ Bovine serum albumin (crystalline) made fluorescent by conjugation with fluorescein-isothiocianate.

The largest molecule which could be shown to diffuse through the cell junctions was serum albumin, 69,000 MW. A synthetic polyaminoacid poly-L-lysin (conjugated with fluorescein-isothianate), of 127,000 MW, the next molecular size tested, did not diffuse beyond the boundaries of the injected cell.

For all the diffusible particles, diffusion seems to be strictly from cell interior to cell interior. There is no detectable leak of any tracer to the exterior, either at the cell surface membranes or at the junctions. These results confirm thus for molecules and ions up to 69,000 MW what the electrical measurements had shown for the smaller ions.

Tissues with Intercellular Connections

How general is intercellular communication?

TABLE 2 gives a list of epithelial cell systems explored to date in our laboratory and summarizes some of their conductive characteristics. All have interconnected cells. The spatial arrangement of the connections differs somewhat in the several systems: In the salivary gland, renal and liver cells, the entire cell system is interconnected, and communication between a given cell and its nearest neighbors is equally good (FIGURE 9). In the urinary bladder and sensory cells, communi-

TABLE 2

Epithelium	Species	Cell Coupling Ratio* V_{II}/V_I	Space Constant* λ 10^{-4} cm)	Normalized Space Constant† $\lambda\ (p/a)^{\frac{1}{2}}$ $(10^{-2}\ cm^{\frac{1}{2}})$	Lumped Specific Core Resistance* R_i (Ω cm)	Membrane Specific Resistance (Ω cm^2)	
						Junctional Maximum‡ R_m^j	Outer Surface§ R_m^b
Salivary gland (1)	*Drosophila* 3rd instar	0.93 ± 0.09	1100 ± 110	50 — 85	150 ± 30	0.3 — 12	**10000** 9000
Salivary gland (2)	*Chironomus* 4th instar	0.8 ± 0.1	750 ± 150	180 — 290	140 ± 40	**0.6 — 1**	3000
Malpighian tubule (2)	*Chironomus*	0.5 ± 0.2	260 ± 140	72	420 — 5900	— 30	
Sensory, Lorenzinian ampulla (2)	*Raja, Mustelus*	0.08 to 0.5					
Urinary bladder (2)	Toad	0.4 to 0.8	18	16 — 33	180	0.02 — ~0.4	$\lesssim$100
Liver (3)	Mouse	0.6					
Liver (4)	Rat	0.8					

* Mean values with their standard deviations.

† p and a are, respectively, perimeter and effective cross-section area of cell chain, not corrected for membrane infoldings. Lower and upper limits, based on an effective cross-sectional area, equal, respectively, to the total cross-section and to the cross-section of the membrane junction (*septate* or *zona occludente*).

‡ Values calculated on the assumption that entire core resistance is due to junctional membranes. Low and high values are based, respectively, on effective junctional areas equal to the areas of the membrane junctions and to total contact areas corrected for membrane infoldings.

§ Corrected for membrane infolding.

Data from (1) Loewenstein & Kanno, 1964; (2) Loewenstein *et al.*, 1965; (3) Penn, 1966; (4) Kanno & Loewenstein, unpublished.

cation is more restricted, manifesting itself in strings of connected cells in the former (FIGURE 10 *A*) and in small clusters of connected cells in the latter (FIGURE 10 *B*) (Loewenstein *et al.*, 1965). However, within their connecting framework, all of these cell systems conform to the scheme of FIGURE 7. Each connected cell ensemble has no significant barriers to ion diffusion in the cell-to-cell direction, as underlined by the low junctional membrane resistances and core resistances, while diffusion in the interior-to-exterior direction is limited by a relatively strong barrier all along the surface of the ensemble (TABLE 2).

The list of tissues of epithelial origin with intercellular communication com-

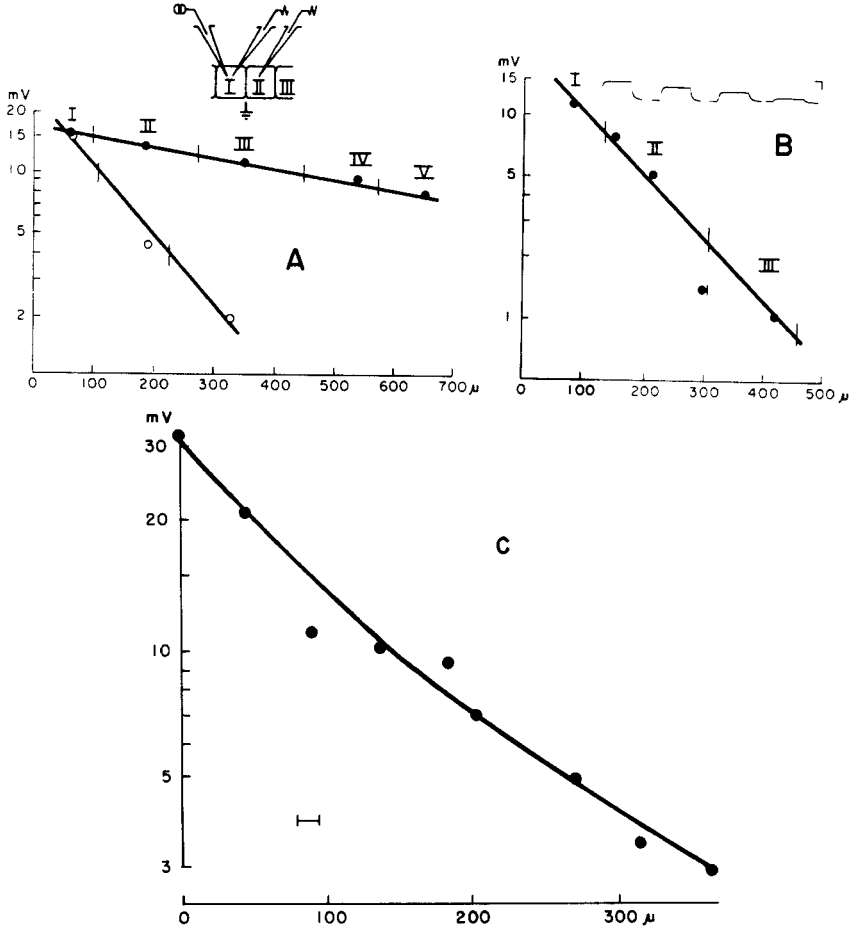

FIGURE 9. Epithelia with "unrestricted" interconnection. Resistive membrane voltages (*ordinates*) recorded at varying distances (*abscissae*) from a current source; procedure as in FIGURE 4. *A*, salivary gland cells (*Chironomus*) at two developmental stages; fourth instar (*solid circles*), prepupa (*open circles*). *B*, Malpighian tubular cells (*Chironomus*). *C*, liver cells (mouse). Vertical lines on curves mark the approximate locations of cell boundaries on *A* and *B*; calibration line gives average cell length on *C*. (From Loewenstein *et al.*, 1965 (*A*, *B*), and Penn, 1966 (*C*).)

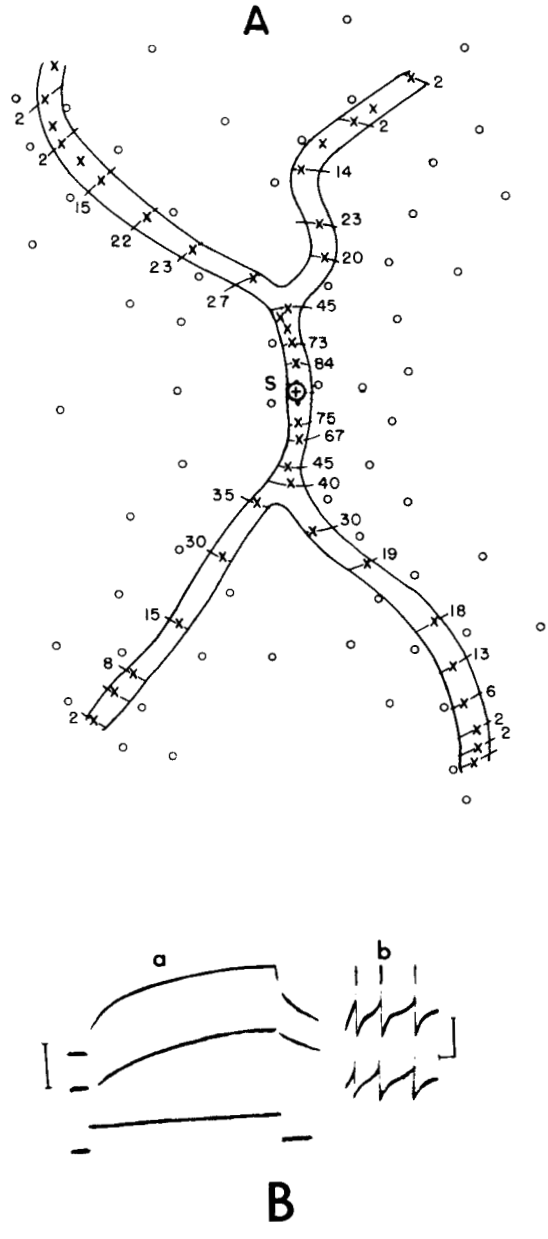

FIGURE 10. Epithelia with restricted intercellular connections.

A, urinary bladder (toad). Current is passed with a microelectrode fixed inside cell *S* and the field of resulting resistive membrane voltage is mapped in the surrounding epithelium. Cells in which no voltage is detectable are marked by open circles. Cells with recordable voltage, by crosses together with the magnitude of voltage. Cell diameter averages approximately 5μ.

B, Sensory epithelium. Lorenzinian ampulla (dogfish). *a*, membrane voltages in two ad-

prises a wide variety of vetrebrate and invertebrate material. In fact, so far we have not come across an epithelial tissue that lacked intercellular communication. Perhaps it may be in order here to add also the neuroglia cells which have low resistance paths (Kuffler & Potter, 1963), and the more special adaptive forms of the electrically transmitting smooth muscle (Burnstock *et al.*, 1963; Nagai & Prosser, 1963; Castillo & DeBell, 1963; Dewey & Barr, 1964; Vayo, 1965) and cardiac muscle fibers (Weidmann, 1952; Woodbury & Crill, 1961; Van der Kloot & Dane, 1964). Intercellular communication seems thus a rather general phenomenon in cell association. The nerve and striated muscle cells with their lack of communication seem the exception rather than the rule. These cells apparently lack over most of their surface the processes required for stable membrane cross-linking (see below) and surround themselves with wide fluid spaces which shunt effectively all electrical cellular cross-talk. However, here and there, certain spots on somas and tips of nerve cells show the character of the more general and, from an evolutionary viewpoint, perhaps more primitive picture, adapted here to electrical signal transmission and synchronization of electrical excitation (Furshpan & Potter, 1959; Tauc, 1959; Watanabe & Bullock, 1960; Hama, 1961; Watanabe & Grundfest, 1961; cf. Grundfest, 1961 & 1966; cf. Eccles, 1961; Robertson, 1960; 1961 & 1963; Hagiwara & Morita, 1962; Bennett *et al.*, 1963 & 1966; Eckert, 1963; Van der Loos, 1963; Martin & Pilar, 1963; Furshpan, 1964; cf. Elbers, 1964). Similarly, spots of this kind are present on certain intracellular membranes of striated muscle (Peachey, 1965; Adrian & Peachey, 1965; Fahrenbach, 1965). This gives a perspective somewhat different from that my neurophysiological colleagues would tend to hold; but I think it is a more realistic one.

Junctional Membrane Structure

The tissues with cell communication listed in TABLE 2 have a common feature at the structural level: they all have cells in close surface contact. In the salivary gland and renal cells, the apposing cell surfaces are joined periodically (*septate junctions*); and in the urinary bladder and liver cells, they are joined at certain regions (*zonas occludente*).

Septate junction. FIGURE 11 shows a diagram of the *Drosophila* salivary gland cell junction as seen in electron micrographs. Over about two-thirds of the length of the junction, the membranes are profusely infolded and intertwined. The intercellular space is here often several thousand Å wide. Over the remainder of the junction, the membranes are aligned in parallel and periodically interconnected. This, the septate junction, is probably the more interesting region in respect to intercellular communication. Here, the intercellular space is at its narrowest; and here are seen also the most striking modifications of surface structure: electron-opaque bridges with what seems an internal polygonal unit structure, linking the two membranes regularly at 150 Å intervals (FIGURE 12) (Wiener *et al.*, 1964). A similar junctional structure is seen in *Chironomus* salivary gland renal cells (S. Bullivant & Loewenstein, unpublished. For morphological aspects of similar junctions in other epithelia, see Wood, 1959; Locke, 1965.).

This junctional region presents itself as a likely site for intercellular communi-

jacent sensory cells (upper two oscilloscope traces; calibration, 20 mV) produced by a current pulse (lower trace; duration, 132 msec.) passed through one cell. Electrode arrangement as in inset of FIGURE 2. *b*, nerve impulses recorded externally with microelectrodes from two sensory nerve fibers (two oscilloscope traces) at the base of adjacent and electrically connected epithelial cells. Note the synchrony of impulses in the two fibers. Calibration, 200 μV; 20 msec. (From Loewenstein *et al.*, 1965.)

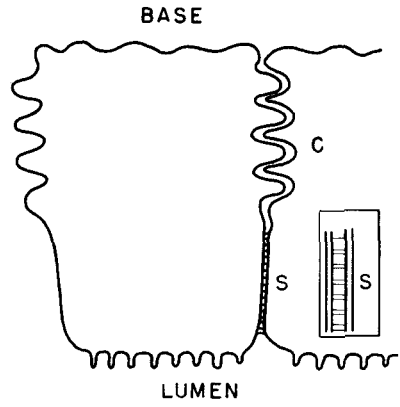

FIGURE 11. Diagram of the regions of cell contact in *Drosophila* salivary gland. *C*, convoluted region at which cell surfaces interdigitate. *S*, septate junction at which membranes are periodically joined.

cation. One may speculate, for instance, that the electron-opaque bridges circumscribe diffusion channels in the cell-to-cell direction. An important point in this connection, which is still unclear, is whether the bridges constitute actual septae continuous along the cell perimeter. If they are continuous, one may possibly think of the septate junction as an alternating sequence of materials of high and low resistivity. Indeed, an arrangement of this sort would make a good ionic coupling device. In the cell-to-cell direction of ion flow, there are many parallel channels lowering the diffusion resistance, while in the direction of intercellular space to exterior, there is a long series of barriers. Such an arrangement provides both the diffusion path and the diffusion barrier required by the results of the electrical and tracer studies. A coupling of this kind implies either that the resistivity of the material of the intercellular space and membranes between bridges be low, while that of the bridges itself be high, or the reverse.

If, on the other hand, the bridges are not continuous along the cell perimeter, but pinlike elements, an attractive picture that suggests itself is that of pins (or pin sub-units) with a core of low resistivity coated with a material of high resistivity. In an arrangement of this kind, each pin (or sub-unit) may be, for example, a water channel sheathed in a circumferential diffusion barrier, patterned, in molecular scale, after certain liquid-crystalline interphases of phospholipids in which molecules appear oriented at certain temperatures in hexagonal arrays of cylinders with central water channels (Luzzati & Husson, 1962). This picture is enticing because the bridges show an internal unit array under the electron microscope with dimensions of similar order as those of the molecular arrays in the phospholipids (FIGURE 12). A coupling device of this sort also provides many parallel diffusion channels and a diffusion barrier to the exterior. But it differs in one important aspect from the coupling with continuous septae. Its diffusion barrier is continuous only for diffusion between the intercellular channels and the intercellular space (and exterior), and not necesarily continuous in the lumen-exterior direction of the intercellular space. The former is the only absolute condition that the experimental results set for a barrier.

It seems fruitless to pursue these speculations into the molecular aspects of membrane permeability of cell junctions until more evidence is available on this point and on the wider problem of the molecular structure of membranes. But we

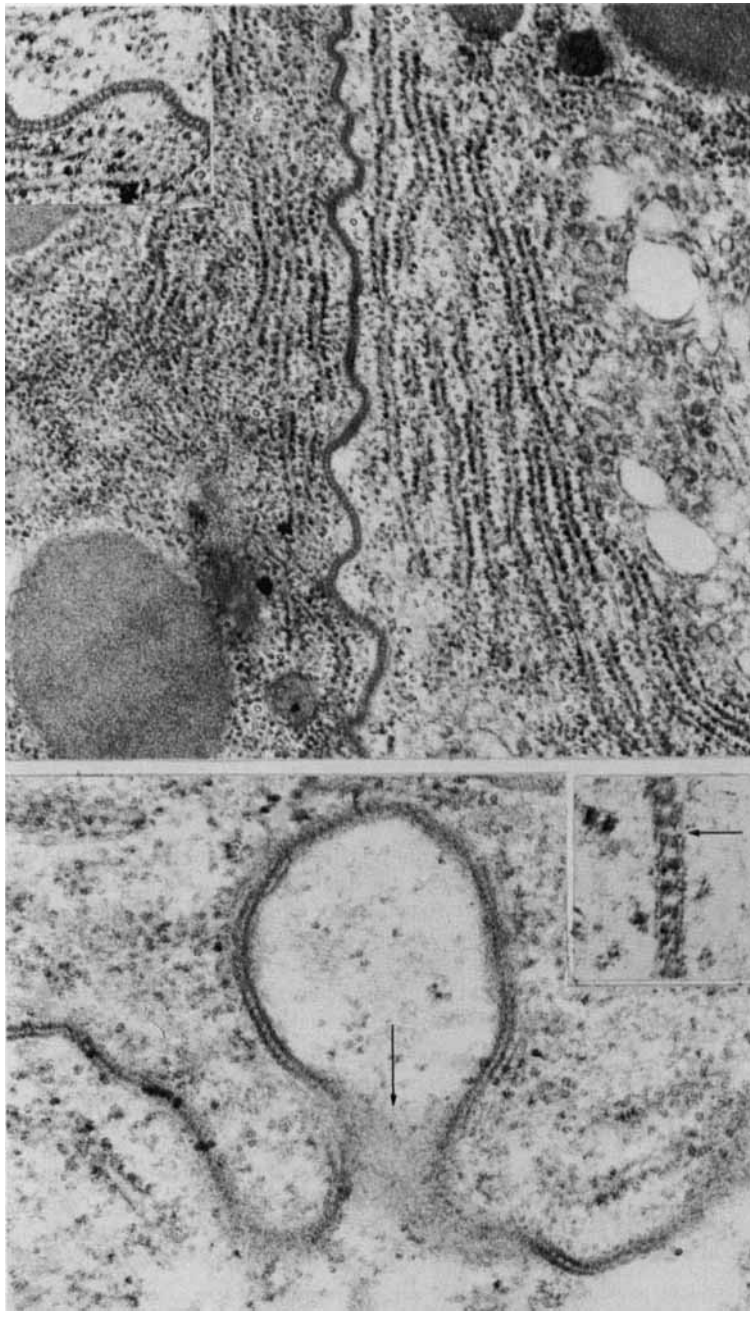

FIGURE 12. Electromicrographs of separate junction (*Drosophila* salivary gland). *Top,* cross-sectional views; × 60,000; inset × 78,000; *bottom,* tangential views; × 90.000; inset, cross-sectional view, × 200,000. (From Wiener *et al.*, 1964.)

may reasonably hope that answers, at least partial ones, concerning the structural sites and identity of particles involved in junctional diffusion will be forthcoming soon from studies combining tracer methods with high resolution techniques for structure. It should be rewarding also, perhaps even in the sight of the wider problem of membrane permeability, to invest further effort in studies of birefringence and X-ray diffraction of membrane junctions.

Zona occludente. The cells in the toad urinary bladder (Peachey & Rasmussen, 1961; Choi, 1963) and in the mouse and rat livers (Benedetti & Emmelot, 1965) and probably also those in the sensory epithelium of Lorenzinian ampullae have membrane junctions of the type that Farquhar and Palade (1963) termed *zona occludente.* At these junctional regions, which encompass membrane areas on the order of 5 μ^2, there is no intercellular space at all discernible under the electron microscope (Farquhar & Palade, 1963). The *zona occludente* is a likely site for intercellular communication. The junctional areas in the *zona occludente* are generally smaller than those of the septate junction; but they are clearly of sufficient magnitude to account for the observed intercellular core resistances on the basis of resistivities of junctional membrane material of the order of 10^{-2} to 10^{-1} Ω cm.^{2} (TABLE 2). For instance, in the toad urinary bladder, a junctional membrane resistivity of 0.02 Ω cm.^{2} accounts for the measured core resistance, if the latter is attributed to the *zona occludente* alone.*

The *zona occludente* is probably functionally similar to the septate junction. One or the other invariably is found when there is intercellular communication in a tissue. This includes also the type of electrically conducting nerve and muscle tissues mentioned before. The class of particles passing through the various junctions may be different, of course. The functional adaptations, in any event, seem different. But it is noteworthy that tangential cuts of *zonas occludente,* electrical nerve synapses, and septate junctions show similarities in shape and dimension of their unit array (see Robertson, 1963; Wiener *et al.*, 1964; Benedetti & Emmelot, 1965).

General Factors in Cell Communication

FIGURE 3 shows, to a first approximation, the equivalent circuit of a communicating longitudinal chain of cells and the factors determining communication: junctional membrane resistance, r_c; surface membrane resistance, r_o; and intercellular space resistance, r_s. A convenient index for cell communication is the ratio of the membrane voltages, V_{II}/V_I, in two adjacent cells resulting from a current flowing through the two. The relation between the factors and the quality of communication is then given by:

$$\frac{V_I}{V_{II}} = 1 + \frac{2\,r_c}{r_p} + \frac{r_c}{r_s}\left(1 + \frac{r_c}{r_p}\right) \qquad (4)$$

where r_p represents the combination of cell surface membrane resistances r_o in cell$_{II}$ in parallel with the entire network to the right of *II*.

Efficient communication between cells requires thus a high r_s and a low r_c. A high r_s apparently did not evolve on the same building blocks as those of the high r_o; as discussed further on, r_s and r_o are affected differently by enzyme action, Ca-removal and other procedures. Instead, the high r_s seems the result of special

* Other regions at which there is close surface contact between cells are the ubiquitous *desmosomes* (cf. Porter, 1956; Fawcett, 1958). These disk-shaped structures are present also in all cell materials dealt with here. It is unlikely, however, that desmosomes are involved in intercellular communication; they are found also in cell associations, such as between glia and nerve cells, which lack electrical connections (Kuffler & Potter, 1964).

processes (of low entropy) binding the cell surface membranes closely together. Close membrane contact is thus in all likelihood always associated with cell communication. The reverse, of course, is not necessarily true, which means only that it is unsafe to rely on morphological criteria alone for identification of communicating junctions.

The second factor, a low r_c, may result from a low membrane resistivity or a large junctional membrane area, or from a combination of both. Communication as efficient as in salivary gland cells is likely to be always associated with low resistivity, because, as discussed above, there is not enough room at cell junctions for the larger surface otherwise required. However, variations within an order of magnitude of r_c, due to differences in junctional surface area in the various junctions, are entirely possible, and at least part of the variations in cell communication in the various tissues may be due to such differences (see TABLE 2). An instructing example is provided by *Chironomous* salivary gland cells. In these cells, junctional membrane area decreases with cell development; and this decrease is associated with a decrease in intercellular communication (FIGURE 9*A*).

Formation of a Cell Junction

The interplay of r_s and r_c in cell communication is seen well during cell division. When a cell divides, a membrane junction forms at the plane of cleavage. We have recently studied the ion communication at such junctions in egg cells of the starfish (*Asterias*) and of the sand dollar (*Echinarachnius*). Electrodes were implanted into a cell on either side of the cleavage plane, and ion communication was probed in the course of cell division (FIGURE 13).

FIGURE 14 illustrates a result in the starfish egg. At the start of cell division, there is full protoplasmic continuity across the cleavage plane, r_c is at its lowest,

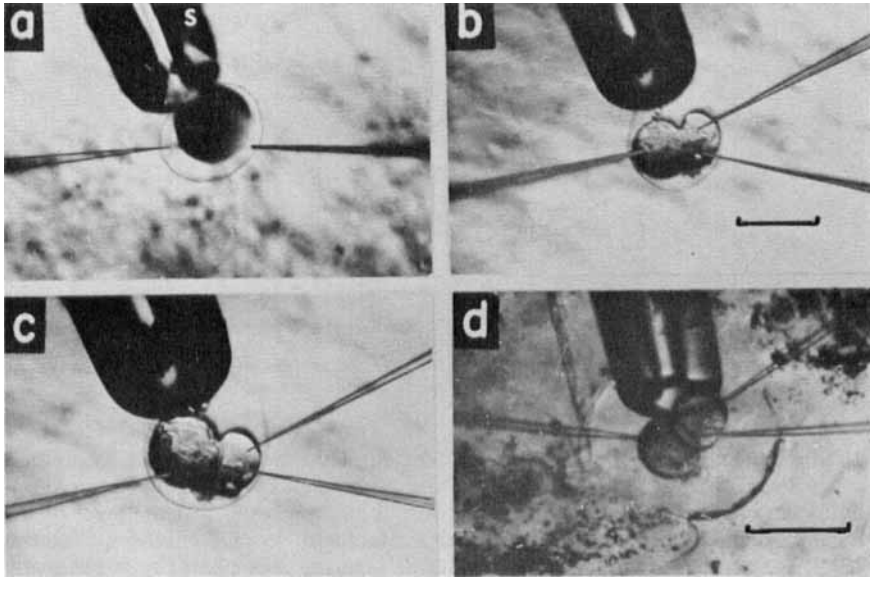

FIGURE 13. A dividing starfish egg cell. Various stages of division of the cell impaled with three microelectrodes. Calibration lines are 100 μ. (From Ashman *et al.*, 1964.)

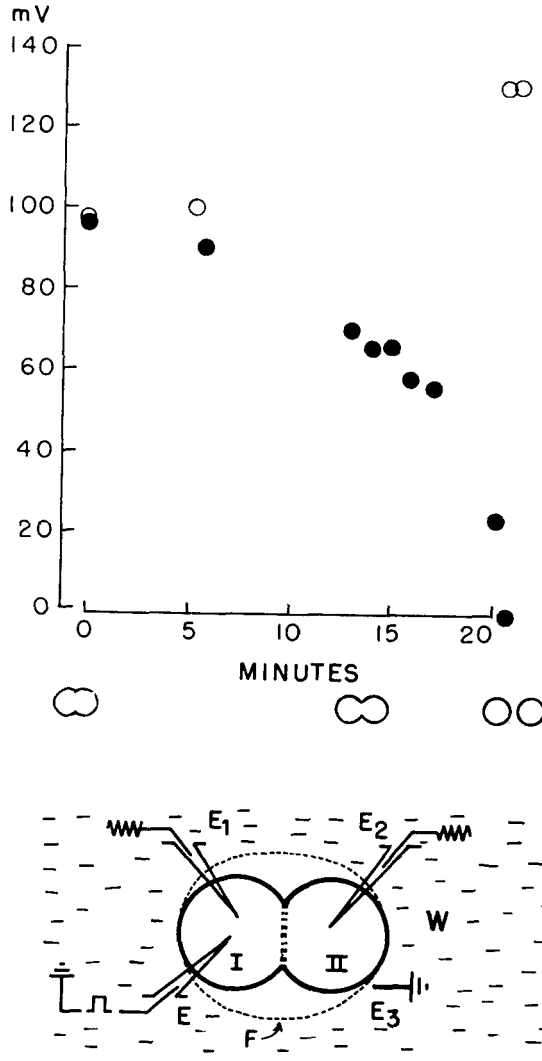

FIGURE 14. Electrical coupling at a forming junction (dividing starfish egg). Current flows from intracellular electrode E to exterior (grounded) and the resulting resistive membrane voltages are recorded with electrodes E_1 and E_2 on either side of the forming junction in blastomere *I* (*open circles*) and *II* (*filled circles*). (From Ashman *et al.*, 1964.)

and the currents are about equal on either side of the cleavage plane. As division proceeds, r_c rises progressively. This phase corresponds with a progressive diminution in effective cross-sectional area of cytoplasmic bridges at the level of the forming membrane junction (see Porter & Machado, 1960; Robbins & Gonatas, 1964, for modes of membrane formation). During this phase, r_s is relatively constant and of a similar high order of magnitude as r_o; in fact, no intercellular space has probably yet formed. At the end of this phase, r_c is relatively high, but

there is still detectable communication between the two cells. In the next and final phase, r_s enters into play as a shunt, as it falls steeply with the completion of the intercellular space and becomes the dominant factor in voltage attenuation. At this time, virtually all ion communication between the cells is lost (Ashman *et al.*, 1964). Essentially similar results are obtained in sand dollar egg cells (Ito & Loewenstein, 1966). A different pattern is found in vertebrate (*Triturus*) egg cells. Here the cells show clear electrical coupling after completion of cell division. There is electrical intercellular coupling even after repeated cell division in the embryonic stage; all cells of the morula are coupled (Ito & Hori, 1966). The significance of this finding cannot be fully evaluated until measurements of specific membrane resistances are made, but it opens the possibility that intercellular communication exists during embryonic development with the interesting implication of a functional role in cellular differentiation (see below).

Interruption of Cell Communication

I turn now to the question of stability of cell communication. This question is obviously linked with that of structural stability of cell junctions, and our first steps were guided by procedures long in use by embryologists for mechanical separation of cells. We were fortunate in that cell communication has much lower safety margins to such procedures than has mechanical cell adhesion. Thus relatively mild procedures could be used. With all of them, interruption of cell communication (hereafter referred to as *functional uncoupling*) was achieved without changes in cell adhesion noticeable by manipulation under the light microscope.

Uncoupling by Ca-removal. Our first attempts were done by removing Ca^{++} from the tissues. It was then from the outset clear that functional uncoupling could be demonstrated only if the effects of Ca^{++} on junctional coupling and on surface membrane permeability differed in rate or reversibility. It turned out that they differed in both, particularly in their reversibility. While the effects on surface membrane permeability were quite reversible, those on junctional coupling were not reversible at all. The two effects could thus be conveniently separated.

FIGURE 15 shows an example of functional uncoupling in a nerve cell junction, the junction between the *Retzius* cells of the leech. These cells are particularly suitable, because, aside from their large size and accessibility, the exchange of ions between cells and bathing fluid is fast (Nicholls & Kuffler, 1964). In the experiment shown, the cells are first bathed in normal saline (FIGURE 15*A*, *left*), then in Ca^{++} free saline, and finally, in normal saline again. FIGURE 15*A*, *right* shows the effects of uncoupling at a time when the surface membrane resistance has fully recovered to normal. Significant here is that while the resistive voltage in cell *II* is smaller than in the control, the resistive voltage in cell *I* is actually larger. This is to be expected upon uncoupling; as the junctional resistance (r_c) increases, a decreasing fraction of the current reaches cell *II*, while an increasing fraction flows through the surface membrane of cell *I* alone (Equation **4**). The junctional resistance increased approximately 3-fold, which is a typical degree of uncoupling in Ca^{++}-free solutions. For more uncoupling, chelating agents had to be used. FIGURE 15*B* shows the results of an experiment in which application of EDTA* produced an approximately 7-fold increase in junctional resistance, enough to cut off nerve impulse interaction between the cells (FIGURE 15 *C*) (Penn & Loewenstein, 1966).

Essentially similar results are obtained in salivary gland cells (Nakas *et al.*, 1966) and in mouse liver cells (Kanno & Loewenstein, unpublished). In these

* Di-sodium ethylene diamino tetraacetate.

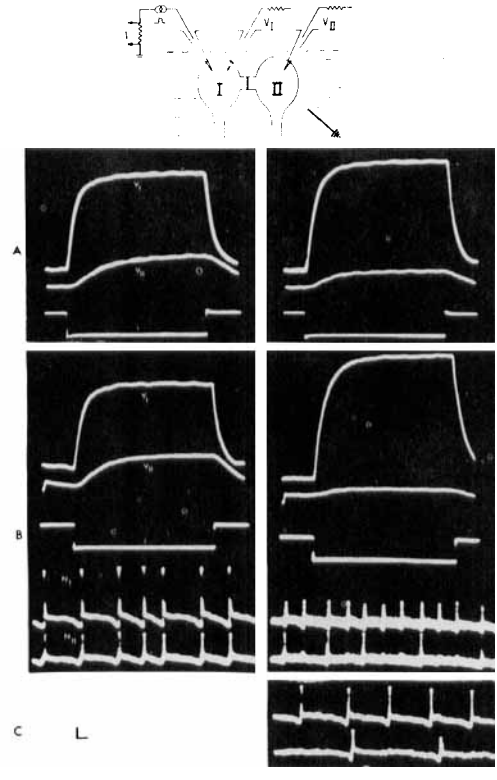

FIGURE 15. Uncoupling of a nerve cell junction by Ca removal (*Retzius* cells, leech). Current is passed between cell interior and exterior, and the resulting resistive membrane voltages V_I and V_{II} are recorded simultaneously in the two cells. *Left column*, V_I, V_{II} and samples of spontaneous nerve impulses N_I, N_{II} in the normally coupled cells; *right column*, after uncoupling of the cells by bathing in preparation *A*, in "Ca^{++}-free" saline; *B*, in saline containing 2.5 mM EDTA; and *C* in 3 mM EDTA. All records of the right column were taken after the preparation was bathed in normal saline for a time sufficient for full reversal of the Ca^{++} effects on the non-junctional surface membranes. Calibration, 10 mV for all records; 20 msec. for *V* and *i*-records; 200 msec. for *N*-records. From Penn & Loewenstein, 1966.)

cell systems, the electrical effects of uncoupling are even more striking, since the cells uncouple from a long chain (in the Retzius cells there are only two cell partners). (FIGURE 16 illustrates this for the case of *Chironomus* gland cells, in which treatment with EGTA† caused virtually complete interruption of intercellular communication.

The stability of junctional communication varies in different tissues. It is higher in the salivary gland (which requires chelating agents for uncoupling) than in the nerve and liver cell junctions (in which mere washing in Ca^{++}-free solution suffices). But in all three tissues, Ca^{++} is clearly an important factor in maintaining cell communication.

Uncoupling by enzyme action. Applications of trypsin to salivary glands (0.05 per cent) lead, within a few minutes, to functional uncoupling (FIGURE 18). The

† Di-sodium ethylene glycol-bis (β-amino ethyl ether)-N′, N′-tetraacetate.

effects of the enzyme on intercellular communication appear to be essentially the same as those of Ca-removal. They are, however, not as clear; trypsin acts also on surface membrane permeability, and this action is largely irreversible and almost as fast as that on communication (Nakas & Loewenstein, 1966).

Uncoupling by hypertonic solution. At higher concentrations and more prolonged treatments than those required for functional uncoupling, chelators and trypsin cause also cell dissociation (hereafter referred to as *mechanical uncoupling*). This suggests that the elements concerned with cell communication and cell adhesion are functionally interrelated, and raises the question of whether functional uncoupling may be produced by mechanical forces alone.

We tried to produce functional uncoupling by pulling cells apart by micromanipulation. These attempts failed; they invariably led to injury of surface

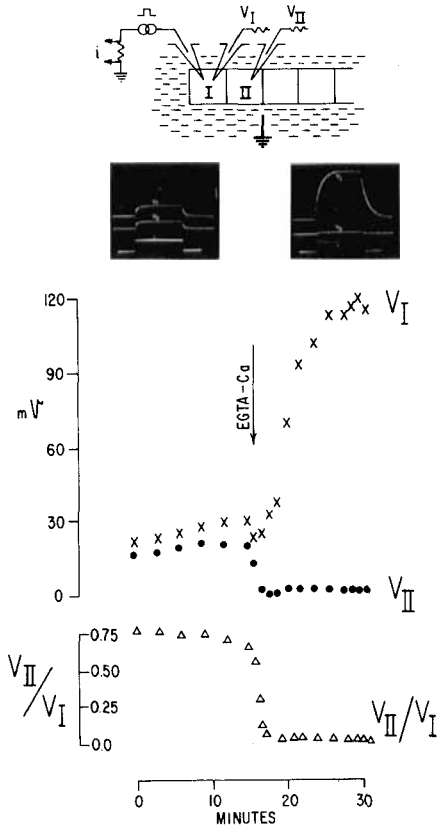

FIGURE 16. Uncoupling of a gland cell junction by Ca removal (*Chironomus* salivary gland). Current pulses (*i*) are passed every ½ or 1 minute and the resulting resistive voltages recorded as diagrammed in upper inset. *Upper ordinates,* membrane voltage, V_I and V_{II} ($i = 5 \times 10^{-8}$ A). *Lower ordinates,* V_{II}/V_I. *At arrow,* the control solution surrounding the preparation is replaced by one containing 1 mM EGTA • 1.5 mM Ca yielding a free Ca^{++} concentration of 0.5 mM. *Insets*: samples of oscilloscope records of membrane voltage (V_I, V_{II}) and membrane current (5×10^{-8} A) before (*left*) and after (*right*) uncoupling. Calibration, 20 mV; current pulse duration, 120 msec. (From Nakas *et al.*, 1966.)

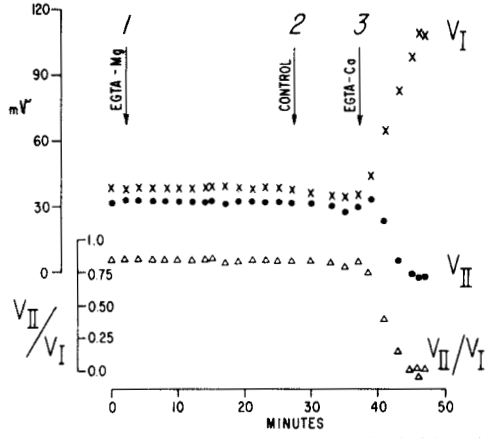

FIGURE 17. Uncoupling prevented in the presence of Mg^{++}. Electrical technique and notations as in FIGURE 16. At *arrow 1*, control solution replaced by a Ca^{++}-free solution containing 2.5 mM EGTA • 2.5 mM $MgCl_2$ (free Mg in excess of 10^{-3} M). *Arrow 2*, back to control solution; *arrow 3*, solution containing 2.5 mM EGTA; 2.5 mM $CaCl_2$ (10^{-4} M free Ca). (From Nakas *et al.*, 1966.)

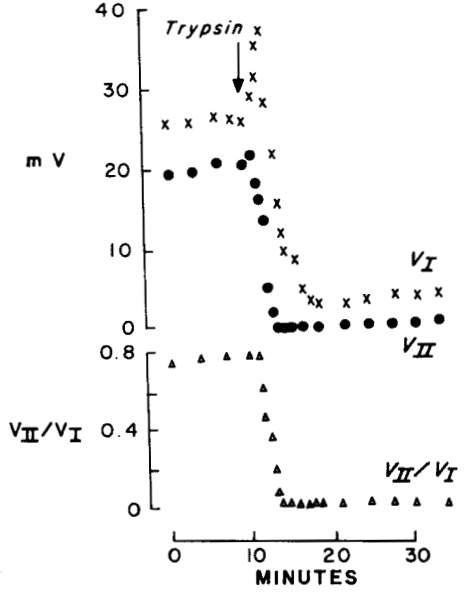

FIGURE 18. Uncoupling by trypsin (0.05 per cent in saline). Notation and procedure as in FIGURE 16. (From Nakas & Loewenstein, 1966.)

membranes. Better results were obtained by soaking the preparations in hypertonic solutions. Under these conditions, unbalanced tensile forces (shear and normal) may be expected to develop at the cell junctions. FIGURE 19 shows an example in which a doubling of tonicity of the bathing fluid by addition of sucrose caused irreversible functional uncoupling in *Chironomus* salivary gland cells. Hypertonicity also causes increase in surface membrane permeability. But this effect is so slow that functional uncoupling may be followed to its peak (FIGURE 19).

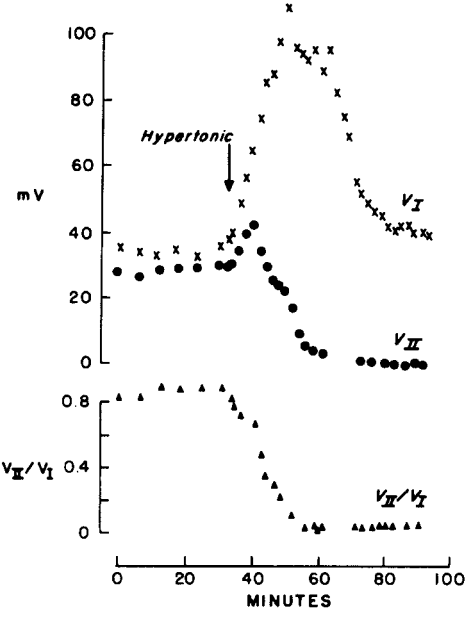

FIGURE 19. Uncoupling in hypertonic solutions (saline twice-osmolar by addition of sucrose). (Fram Nakas & Loewenstein, 1966.)

Role of Ca

In the course of uncoupling, the junctional membrane goes through a striking transformation in resistivity which is of interest in itself. The junctional membranes, highly permeable in the normally connected cells, become relatively impermeable, as is clear from the rise in V_I. For this sealing process, Ca^{++} is required. This first became apparent in experiments in which chelator-Ca complexes were employed for uncoupling. It was then observed that when the concentrations of free Ca^{++} were above 10^{-4} M, uncoupling was accompanied by sealing of the junctional membrane. But when they fell below 10^{-4} M, sealing was invariably absent (Nakas & Loewenstein, 1966). Mouse liver cells behaved similarly (Kanno & Loewenstein, unpublished). To round out the picture, it was then only necessary to show that subsequent addition of Ca^{++} did produce membrane sealing, as exemplified in FIGURE 20.

An experiment that shows this action of Ca^{++} most directly is illustrated in FIGURE 21. Here a large hole is made in the surface membranes of cells *I* and *III* belonging to a connected chain so as to put the junctional membranes in contact

with the bathing fluid. In Ca^{++} concentrations below 10^{-4} M, the system is leaky; membrane resistance is immeasurably low (FIGURE 21, c_{II}). In higher Ca^{++} concentrations, the resistance is of the order of 10^6 Ω; cell *II* has sealed itself off (d_{II}). This is almost entirely due to sealing of the junctional membranes: the perforated cells stay as leaky as before (d_I); and the effects of Ca^{++} on surface membrane permeability are negligible by comparison b_I, b_{II}).

Ca^{++} appears thus to enter twice in the junctional processes: once as a structural element in the adhesive processes linked with cellular communication, and again in the processes of transformation of junctional membrane permeability. Mg^{++} substitutes for Ca^{++} in the former (FIGURE 17) as well as in the latter process.

The capacity of connected cell ensembles of sealing their interiors off from a damaged cell member would seem to offer a simple protective means against injury. This should be especially important in epithelia located at the periphery of organisms. In addition, some observations on injured heart muscle dating back as far as the last century (Engelmann, 1877; Rothschuh, 1951; Weidmann, 1952; Délèze, 1965) may fit in this teleological parenthesis. These observations deal with a peculiar capacity of injured heart muscle to "heal" – a capacity entirely lacking in skeletal muscle. The "healing" may perhaps now be interpreted as a phenomenon of junctional membrane sealing.

A Functional Picture of a Membrane Junction

One may try now to piece together a picture of the cell junction on the basis of the available data. The following points serve as guideposts: (1) Cell unity

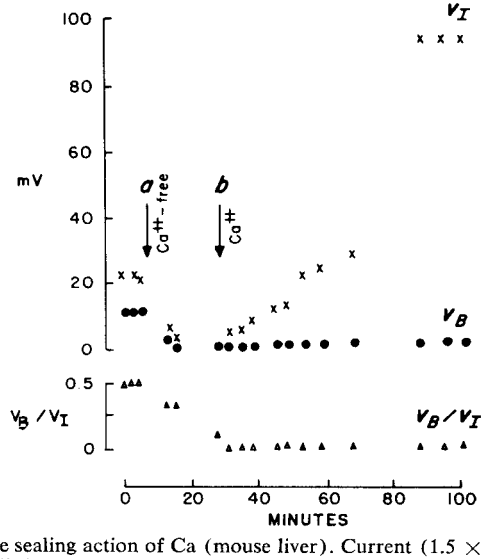

FIGURE 20. The sealing action of Ca (mouse liver). Current (1.5×10^{-7} A) is passed with an electrode in cell *I*, and the resulting resistive membrane voltages are recorded with electrodes in this cell and another one (*B*) 2 to 4 cells away. At *arrow 2*, preparation is bathed in Ca^{++}-free saline to uncouple the cell system; at *b*, in saline containing 2.5 mM Ca. Membrane resistance is tested at end of experiment also in cell *B* (not shown on this figure) and is found to be similar to that of cell *I*.

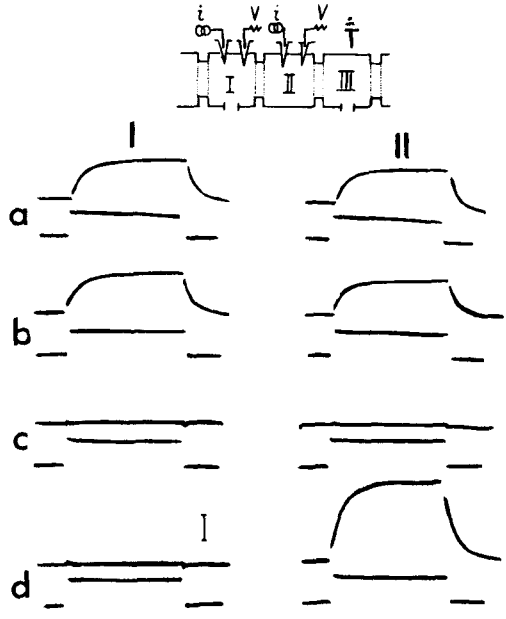

FIGURE 21. Junctional membrane sealing. Current is passed either from inside of cell *I* or from inside of cell II of a cell chain (salivary gland cells). Column *I* shows the resistive membrane voltages (upper oscilloscope trace) as recorded in cell *I* when current (lower oscilloscope trace, 5×10^{-8} A) is passed from inside cell *I*. *Column II* shows the voltages recorded in cell *II* when current is passed from inside cell *II*. *a*, intact cell chain in normal saline containing 10^{-3} M Ca; *b*, in saline containing 10^{-5} M Ca^{++}; *c*, after perforation cells *I* and *II*, in saline with 10^{-5} M Ca^{++}; *d*, in saline with 10^{-3} M Ca^{++}.

is absent in function in the connected system, but not in structure. All essential structural elements of the cell, including the membranes at the junctional surfaces, appear to be present. When disjoined, the cells survive as structural units and become units even in the functional sense, as is plain in many ways from cell culture and embryological work. (2) The functional junction between cell membranes is a highly structured thing, not a simple apposition. This is particularly clear in the septate junction with its orderly array. A high degree of order is also suggested by the irreversibility of the uncoupling process. The membrane is preserved as surface barrier all around the cell upon uncoupling, as is clear from the electrical measurements; yet, once the membranes are uncoupled, and regardless of the procedures used in uncoupling, junctional communication is not restored by mere proximity of the membranes. (3) Some form of surface continuity exists between cells, insulating the interior of the connected system from the exterior, as is shown by the electrical measurements and studies with fluorescent tracers. This surface insulation is interdependent with cell adhesion; both are destroyed by the same agents. The elements in insulation and in adhesion, however, do not seem to be identical, since their stabilities are different. (4) The normally highly permeable junctional membrane transforms into one of low permeability in the presence of Ca^{++}. Upon such transformation, the junctional membranes are no longer distinguishable from the surface membranes as far as their total ion conductances are concerned. (5) The junctional membranes are

normally in contact with a medium of low Ca^{++} concentration on their cytoplasmic sides (see, for instance, Keynes & Lewis, 1956; Hodgkin & Keynes, 1957). In all likelihood this is also the case at their other (external) sides, because the system is insulated from the extracellular fluid, and there is unlikely to be a separate ion compartment between the highly conductive and non-rectifying junctional membranes. This is the most obvious situation of contrast with the non-junctional membranes.

A picture that fits these points is diagrammed in FIGURE 22. It depicts a *junctional unit* consisting of three principal elements: (i) the junctional membranes, *C*; (ii) the surface diffusion barrier, *S*; and (iii) the element of structural rigidity and adhesion, *A*.

With respect to *C*, the hypothesis will be tentatively made that its permeability is chiefly controlled by Ca^{++}. With respect to *S*, it is assumed that its integrity depends on that of *A*. No special assumption need be made for *S*; cell adhesion is known to depend on Ca^{++} and to be impaired by trypsin (Chambers, 1940; Holtfreter, 1947; Moscona, 1952).

In the light of this picture, the experimental results described in this paper may be interpreted as follows: Permeability of the junctional membranes is normally high, because of a low Ca content in these membranes. Reduction of adhesive forces between cells by trypsin, Ca-removal or, directly, by mechanical forces opposing adhesion, leads to discontinuity of the surface barrier and, consequently, to contact between junctional membranes and extracellular fluid. If this fluid contains sufficient Ca^{++}, as it normally does, the junctional membranes become relatively impermeable.

The picture of the *junctional unit* (many parallel units make up a membrane junction) is a purely functional one. At the present stage, one may at best guess at the structural equivalents of some of its elements (see page 454). In searching for a control element of junctional permeability, the most obvious one, calcium, was chosen. There may be others, of course. For example, the high concentration of K^+ on either side of the junctional membranes, which is another obvious situation of contrast with respect to the non-junctional membranes, may conceivably contribute to the high ion permeability in some cases. Cell membrane conductance increases generally when the extracellular K^+ concentration is made as high as the intracellular one (skeletal muscle, Hodgkin & Horowicz, 1959; nerve, E. Rojas, personal communication; heart muscle, D. Noble, personal communication); but the increase is at most 6-fold, in all cases far from sufficient to account for a difference in permeability of four orders of magnitude between junctional and non-junctional membranes. Sequestering of Ca^{++}, on the other hand, causes

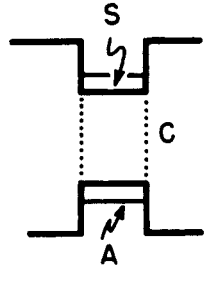

FIGURE 22. Junctional unit. See text.

such increases in membrane permeability; and, conversely, application of Ca to junctional membranes causes such reductions in permeability (FIGURES 20, 21).

Some Functional Implications of Cell Communication

The curious lesson from the results on intercellular communication is that the entire connected cell system, rather than the single cell, constitutes the functional unit. This qualification of classical cell theory came as a rather unexpected by-product of our work. Probably the functional adaptation here is one that allows the cell system to operate in concert. The junctional membranes are permeated by particles of molecular weights at least as high as 69,000. Hence, many of the ions and molecules normally present in the cells, may flow from cell to cell. Junctional communication provides, thus, a means for tissue homeostasis and functional control. There would seem to be even enough room for genetic and hormonal information to flow from cell to cell, exerting direct functional control over the cell system. This may conceivably be at the root of cellular differentiation during embryogenesis and in the maintenance of this differentiation during the adult life of the cell.

Tissue growth. Cancer. I should like to end my story by dealing with a kind of information flow in which intercellular communication is almost certainly implicated. The nature of the information in this case is not known, but its effects are sufficiently clear to serve as indices.

It has long been known that cells react to each other when they establish contact. There are many manifestations of such contact interactions. A striking one is the harmonious growth of organs and tissues. Such growth requires, among other things, that cells distinguish each other according to kind and stop moving and dividing at the right place. An instructive example is the movement of two fringes of epidermal cells over a wound; the movement stops when the fringes meet (Lash, 1955). Another one is the behavior of cultured cells growing on a glass surface. The cells stop moving (and dividing) when they touch each other; and stop only then (Abercrombie & Heaysman, 1954; Weiss, 1958). Some kind of signal must be transmitted from cell to cell upon contact.

The question is then whether intercellular communication of the kind described in this paper is involved in the transmission of such signals. If substances are the signals, as they almost certainly must be, and these substances diffuse from cytoplasm to cytoplasm, the junctional membranes, with their high permeability to a wide range of particles, offer a possible diffusion path. This suspicion is nursed further by a number of old observations in embryology showing impairment of normal tissue growth (cf. Weiss, 1958; Harris, 1964) precisely under conditions that will lead to impairment of intercellular communication. For instance, cells dissociated under conditions that make r_s a shunt and r_c a diffusion barrier (Equation 4) do not form normal tissues.

A direct approach to the question seems hopeless until specific signal substances are identified. But one may try an indirect approach and see whether intercellular communication is altered in situations of uncontrolled cellular growth. The most notorious lack of growth control occurs in cancer cells. Cancer cells, unlike normal cells, neither stop moving nor dividing upon cellular contact, as is seen particularly clearly in cultured cancer cells growing on glass plates (Abercrombie *et al.*, 1957; Rubin, 1961; Dulbecco, 1963; Berwald & Sachs, 1963). The question becomes then whether there are changes in intercellular communication detectable in cancer. Electrical techniques of the sort described above are well suited to test this question. They are readily applicable to many cell systems and

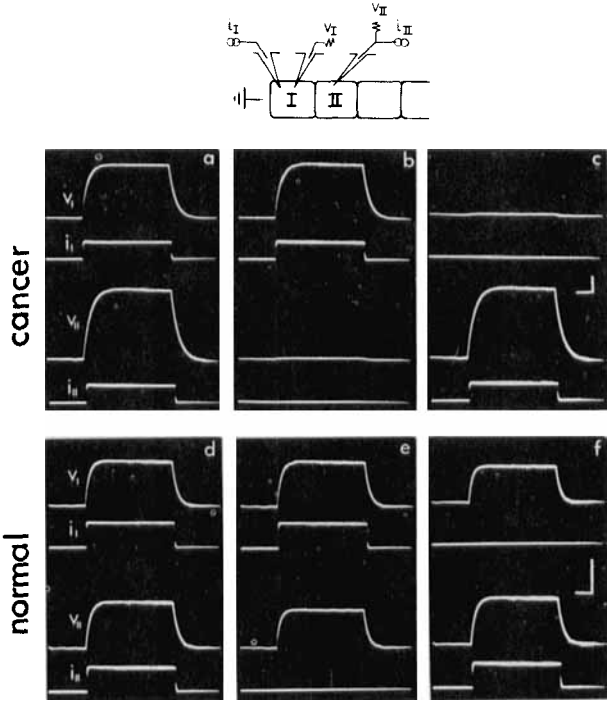

FIGURE 23. Lack of electrical communication in cancer cells (Novikoff rat liver cancer). *a*, to test integrity of cell surface membranes, current ($i_I = 9 \times 10^{-9}$ A) is passed from inside cell *I*, and the resulting resistive voltage (V_I) is recorded in this cell (upper two oscilloscope traces). Current is then passed through adjacent cell *II* ($i_{II} = 1.8 \times 10^{-8}$ A), and voltage recorded in cell *II* (lower two traces). Then, to test intercellular communication, current is passed alternatively from cell *I* (*b*) and from cell *II* (*c*), and the voltages are recorded simultaneously in the two cells.

For a comparison, a similar sequence is shown in *d–f* for normal rat liver ($i_I = 1.3 \times 10^{-7}$ A; $i_{II} = 2.8 \times 10^{-7}$ A). Calibration, voltage 10 mV; time, 20 msec. Note that the current used was much larger in the normal cells; the input resistance of the normal cells were 1.8×10^5 Ω, and in the cancer cells 6.4×10^6 (*I*) and 8.6×10^6 Ω (*II*). Electrical arrangement is essentially the same as in the experiments of preceding illustrations, except that here in cell *II* one microelectrode is connected to a balanced bridge circuit and serves for both passing of current and recording of voltage. (From Loewenstein & Kanno, 1966.)

provide quantitative information. All that is required is a cancer material with cells sufficiently large and accessible for intracellular measurements, and one whose normal cell counterpart presents good intercellular communication.

A suitable material is provided by liver cells of the mouse and rat. This is the material that Y. Kanno and I have recently used. We examined a variety of liver cancers covering a broad spectrum of growth rates, invasiveness, and cellular differentiation*. All lacked the intercellular communication characteristic of normal liver. While normal liver cells communicate through low cell-to-cell resistance, and communication is detectable electrically over distances many cells long, as shown by my colleague R. Penn (1966) (FIGURES 9*C* and 23 *e, f*), cancer

* The following liver cancers were used. Rat, primary: Azo-die induced (Sorof). Rat, transplantable: Novikoff; Morris minimal deviation Nos. 7787 and 7793.

cells have no detectable communication at all (FIGURE 23*b*, *c*) (Loewenstein & Kanno, 1966). As far as their conductive membrane properties are concerned, cancer cells resemble normal cells that have been artificially uncoupled (see foregoing section). Their ratio V_{II}/V_I is less than 0.002, the limit of resolution of our method, as against 0.8 in normal liver cells; and their effective surface membrane resistance is two orders of magnitude higher than in the normal cells. The differences are so large that identification of cancer cells can be done with ease at the cellular level.

Cancer cells are thus sealed off from the exterior by a diffusion barrier of high resistance which, unlike that of the normal cell, extends all around the cell surface. The cancer cell is then functionally a rather independent unit which cannot engage in the cross-talk possible in its normal counterpart.

CONCLUSIONS

The junctional membranes in epithelial cells (salivary gland, renal, urinary bladder, sensory, and liver cells) are highly permeable structures. Their conductance is 100 to 0.1 mho/cm^2, in all cases at least 4 orders of magnitude greater than that of the non-junctional surface membranes. The cells form communicating systems in which ions and molecules of molecular weight up to at least 69,000 move freely from one cell to another but do not leak appreciably to the exterior. The general functional picture is that of a connected cell system with a fairly continuous cytoplasmic core bounded by a surface barrier to diffusion continuous all along the system (FIGURES 7 and 22). A primary factor in controlling junctional membrane permeability is Ca^{++}. Ca^{++} concentration is normally low on both sides of the junctional membranes. When its concentration is raised above 10^{-4} M, the junctional membranes become as impermeable as the non-junctional ones; each cell seals itself off as a unit. (Mg^{++} substitutes for Ca^{++} in this action.) As might be expected, cell communication depends on the stability of the elements binding the cells together. These elements have a high degree of structural order (*septate junction, zona occludente*). Ca^{++} is a factor in their stability – and this quite apart from its direct role in junctional membrane permeability. (Here too, Mg^{++} substitutes for Ca^{++}.) Withdrawal of Ca from the structural elements, or other procedures impairing their stability, such as trypsin digestion or application of anisotonic solutions, cause interruption of communication.

Many of the ions and molecules, including metabolites, normally present in cells fall within the size range of substances shown to permeate the junctional membranes. Cellular interconnection thus seems to provide a means for functional regulation through direct cell-to-cell diffusion of control substances. A case in point may well be the control of tissue growth and differentiation: cancer cells (liver) lack intercellular communication.

References

ABERCROMBIE, M. & E. M. HEAYSMAN. 1954. Social behavior of cells in tissue culture. II. Monolayering of fibroblasts. Exp. Cell Res. **6**: 293–306.

ABERCROMBIE, M., E. M. HEAYSMAN & H. M. KARTHAUSER. 1957. Social behavior of cells in tissue culture. III. Mutual influence of sarcoma cells and fibroblasts. Exp. Cell Res. **13**: 276–291.

ADRIAN, R. H. & L. D. PEACHEY. 1965. The membrane capacity of frog twitch and slow muscle fibers. J. Physiol. (London) **181**: 324–336.

ASHMAN, R. F., Y. KANNO & W. R. LOEWENSTEIN. 1964. The intercellular electrical coupling at a forming membrane junction in a dividing cell. Science **145**: 604–605.

BENEDETTI, E. L. & P. EMMELOT. 1965. Electron microscopic observations on negatively stained plasma membranes isolated from rat liver. J. Cell Biol. **26**: 299–304.

BENNETT, M. V. L., E. ALJURE, Y. NAKAJIMA & G. D. PAPPAS. 1963. Electrotonic junctions between teleost spinal neurons: Electrophysiology and ultrastructure. Science **141**: 262–264.

BENNETT, M. V. L., Y. NAKAJIMA & G. D. PAPPAS. 1966. Physiology and ultrastructure of electrotonic junctions. I. Supramedullary neurons. J. Neurophysiol. (In press).

BERWALD, Y., & L. SACHS. 1963. *In vitro* cell transformation with chemical carcinogens. Nature **200**: 82–1184.

BURNSTOCK, G., M. E. HOLMAN & C. L. PROSSER. 1963. Electrophysiology of smooth muscle. Physiol. Rev. **43**: 482–527.

CASTILLO, J. DEL, J. T. DEBELL & V. SÁNCHEZ. 1963. Electrical behavior of ascaris muscle cells. Fed. Proc. **19**: 159.

CHAMBERS, R. 1940. The relation of extraneous coats of organization and permeability of cell membranes. Cold Spring Harbor Symp. Quant. Biol. **8**: 144–152.

CHOI, J. K. 1963. The fine structure of the urinary bladder of the toad, *Bufo marinus*, J. Cell Biol. **16**: 53–72.

DÉLÈZE, J. 1965. *In* Electrophysiology of the Heart. Taccardi & Machetti, Eds. Pergamon Press, Inc., Oxford, England.

DEWEY, M. M. & L. BARR. 1964. A study of the structure and distribution of the nexus. J. Cell Biol. **23**: 553–585.

DULBECCO, R. 1963. Transformation of cells in vitro by viruses. Science **142**: 932–936.

ECCLES, J. C. 1961. The mechanism of synaptic transmission. Ergebn. Physiol. Biol. Chem. und Exp. Pharmakol. **51**: 300–430.

ECKERT, R. 1963. Electrical interaction of paired ganglion cells in the leech. J. Gen. Physiol. **46**: 573–587.

ELBERS, P. F. 1964. The cell membrane: Image and interpretation. Recent Progr. in Surface Science **2**: 443–503.

ENGELMANN, T. W. 1877. Vergleichende Untersuchungen zur Lehre von der Muskel- und Nervenelektricität. Pflüg. Arch. ges. Physiol. **15**: 116–148.

FAHRENBACH, W. 1965. Sarcoplasmic reticulum: Ultrastructure of the triadic junction. Science **147**: 1308–1310.

FARQUHAR, M. G. & G. E. PALADE. 1963. Junctional complexes in various epithelia. J. Cell Biol. **17**: 375–412.

FAWCETT, D. W. 1958. Structural specialization of the cell surface. In Frontiers in Cytology. 19 pp. S. L. Palay, Ed. Yale University Press. New Haven, Conn.

FURSHPAN, E. J . 1964. Electrical transmission at an excitatory synapse in a vetrebrate brain. Science **144**: 878.

FURSHPAN, E. J. & D. D. POTTER. 1959. Transmission at the giant motor synapses of crayfish. J. Physiol. (London) **145**: 289–325.

GRUNDFEST, H. 1961. General physiology and pharmacology of junctional transmission. *In* Biophysics of Physiological and Pharmacological Actions. A. Shanes, Ed. AAAS Publ. No. 69, 322 pp.

GRUNDFEST, H. 1966. Heterogeneity of excitable membrane: Electrophysiological and pharmacological evidence and some consequences. Ann. N. Y. Acad. Sci. (This volume.)

HAGIWARA, S. & H. MORITA. 1962. Electrotonic transmission between two nerve cells in leech ganglion. J. Neurophysiol. **25**: 721–731.

HAMA, K. 1961. Some observations on the fine structure of the giant fibers of the crayfishes (*Cambarus virilus* and *Cambarus clarkii*) with special reference to the submicroscopic organization of the synapses. Anat. Rec. **141**: 275–293.

HARRIS, M. 1964. Cell Culture and Somatic Variation. Holt, Rinehart and Winston, Inc. New York, N. Y.

HODGKIN, A. L. & P. HOROWICZ. 1959. The influence of potassium and chloride ions on the membrane potential of single muscle fibres. J. Physiol. (London) **148**: 127–160.

HODGKIN, A. L. & R. D. KEYNES. 1957. Movements of labelled calcium in squid giant axon. J. Physiol. (London) **138**: 253–281.

HODGKIN, A. L. & W. A. H. RUSHTON. 1946. The electrical constants of a crustacean nerve fibre. Proc. Roy. Soc. London, Series B **133**: 444.

HOLTFRETER, J. 1947. Significance of the cell membrane in embryonic processes. Ann. N. Y. Acad. Sci. **49**: 709–755.

ITO, S. & N. HORI. 1966. Electrical characteristics of *Triturus* egg cells during cleavage. J. Gen. Physiol. **49**: (In press).

ITO, S. & W. R. LOEWENSTEIN. 1966. The formation of a cell junction. J. Gen. Physiol. (In press).

KEYNES, R. D. & P. R. LEWIS. 1956. The intracellular calcium contents of some invertebrate nerves. J. Physiol. (London) **134**: 399–407.

KUFFLER, S. W. & D. D. POTTER. 1964. Glia in the leech central nervous system: Physiological properties and neuron-glia relationships. J. Neurophysiol. **27**: 290–320.

LASH, J. W. 1955. Studies on wound closure in Urodelis. J. Exp. Zool. **128**: 13–28.

LOCKE, M. 1965. The structure of septate desmosomes. J. Cell Biol. **25**: 160–169.

LOEWENSTEIN, W. R. & Y. KANNO. 1964. Studies on an epithelial (gland) cell junction. I. Modifications of surface membrane permeability. J. Cell. Biol. **22**: 565–586.

LOEWENSTEIN, W. R. & Y. KANNO. 1966. Lack of intercellular communication in cancer cells. Nature **209**: 1248–49.

LOEWENSTEIN, W. R., S. J. SOCOLAR, S. HIGASHINO, Y. KANNO & N. DAVIDSON. 1965. Intercellular communication: renal, urinary bladder, sensory, and salivary gland cells. Science **149**: 295–298.

LUZZATI, V. & F. HUSSON. 1962. The structure of the liquid-crystalline phases of lipid-water systems. J. Cell Biol. **12**: 207–219.

MARTIN, A. R. & G. PILAR. 1963. Dual mode of synaptic transmission in the avian ganglion. J. Physiol. (London) **168**: 443.

MOSCONA, A. A. 1952. Cell suspension from organ rudiments of chick embryo. Exp. Cell Res. **3**: 535–539.

NAGAI, T. & C. L. PROSSER. 1963. Electrical parameters of smooth muscle cells. Am. J. Physiol. **204**: 915–924.

NAKAS, M., S. HIGASHINO & W. R. LOEWENSTEIN. 1966. Uncoupling of an epithelial cell membrane junction by calcium-ion removal. Science **151**: 89–91.

NAKAS, M. & W. R. LOEWENSTEIN. 1966. Studies on an epithelial (gland) cell junction. III. Junctional uncoupling. J. Cell Biol. (In press).

NICHOLLS, J. G. & S. W. KUFFLER. 1964. Extracellular space as a pathway for exchange between blood and neurons in the central nervous system of the leech: ionic composition of glial cells and neurons. J. Neurophysiol. **27**: 645–671.

PEACHEY, L. D. 1965. The sarcoplasmic reticulum and transverse tubules of the frog's sartorius. J. Cell Biol. **25**: 209–321.

PEACHEY, L. D. & H. RASMUSSEN. 1961. Structure of the toad's urinary bladder as related to its physiology. J. Biophysic. and Biochem. Cytol. **10**: 529.

PENN, R. D. 1966. Ionic communication between liver cells. J. Cell Biol. **29**: (In press).

PENN, R. D. & W. R. LOEWENSTEIN. 1966. Uncoupling of a nerve cell membrane junction by calcium-ion removal. Science **151**: 88–89.

PORTER, K. R. 1956. Observations on the fine structure of animal epidermis. *In* Proceedings of Third International Conference on Electron Microscopy. 539 pp. R. Ros, Ed. Royal Microscopical Society. London.

PORTER, K. R. & R. D. MACHADO. 1960. Studies on the endoplasmic reticulum. IV. Its form and distribution during mitosis in cells of onion root tip. J. Biophysic. and Biochem. Cytol. **7**: 167–180.

ROBINS, E. & N. K. GONATAS. 1964. The ultrastructure of a mammalian cell during the mitotic cycle. J. Cell Biol. **21**: 425–463.

ROBERTSON, J. D. 1960. The molecular structure and contact relationship of cell membranes. Progr. Biophysics and Biophysic. Chem. **10**: 343–389.

ROBERTSON, J. D. 1961. Ultrastructure of excitable membranes and the crayfish median-giant synapse. Ann. N. Y. Acad. Sci. **94**: 339.

ROBERTSON, J. D., T. S. BODENHEIMER & D. E. STAGE. 1963. The ultrastructure of Mauthner cell synapses and nodes in goldfish brains. J. Cell Biol. **19**: 159–199.

ROTHSCHUH, K. E. 1951. Über den funktionellen Aufbau des Herzens aus elektrophysiologischen Elementen und über den Mechanismus der Erregungsleitung im Herzen. Pflüg. Arch. ges. Physiol. **253**: 238–251.

RUBIN, H. 1961. Influence of tumor virus infection on the autogeneity and behavior of cells. Cancer Res. **21**: 1244–1253.

TAUC, L. 1959. Neurophysiologie comparée. Interaction non synaptique entre deux neurones adjacents du ganglion abdonimal de l'Aplysie. C. R. Acad. Sci. **248**: 1857–1859.

VAN DER KLOOT, W. G. & B. DANE. 1964. Conduction of the action potential in the frog ventricle. Science **146**: 74–75.

VAN DER LOOS, H. 1963. Fine structure of synapses in the cerebral cortex. Z. Zellforsch. **60**: 815.

VAYO, H. W. 1965. Determination of the electrical parameters of vertebrate visceral smooth muscle. J. Theoret. Biol. **9**: 263–277.

WATANABE, A. & T. H. BULLOCK. 1960. Modulation of activity of one neuron by subthreshold slow potentials in another in lobster cardiac ganglion. J. Gen. Physiol. **43**: 1031–1045.

WATANABE, A. & H. GRUNDFEST. 1961. Impulse propagation at the septal and commissural junctions of crayfish lateral giant axons. J. Gen. Physiol. **45**: 267–308.

WEIDMANN, S. 1952. The electrical constants of Purkinje fibres. J. Physiol. (London) **118**: 348–360.

WEISS, J. 1958. Cell contact. International Rev. Cytol. **7**: 391–423.

WIENER, J., D. SPIRO & W. R. LOEWENSTEIN. 1964. Studies on an epithelial (gland) cell junction. II. Surface structure. J. Cell Biol. **22**: 587–598.

WOOD, R. L. 1959. Intercellular attachment in the epithelium of *Hydra* as revealed by electron microscopy. J. Biophysic. and Biochem. Cytol. **6**: 343–351.

WOODBURY, J. W. & W. E. CRILL. 1961. *In* Nervous Inhibition. E. Florey, Ed. Pergamon Press. New York, N. Y.